Applied Physics Letters

Surface transfer doped diamond diodes with metal oxide passivation and field-plate

Cite as: Appl. Phys. Lett. **122**, 093503 (2023); https://doi.org/10.1063/5.0128490
Submitted: 28 September 2022 • Accepted: 16 February 2023 • Published Online: 28 February 2023
Published open access through an agreement with JISC Collections

Rebecca J. Watkins, Calum S. Henderson, Alexander C. Pakpour-Tabrizi, et al.

Applied Physics Letters ARTICLE scitation.org/journal/apl

Surface transfer doped diamond diodes with metal oxide passivation and field-plate

Cite as: Appl. Phys. Lett. **122**, 093503 (2023); doi: 10.1063/5.0128490
Submitted: 28 September 2022 · Accepted: 16 February 2023 ·
Published Online: 28 February 2023

Rebecca J. Watkins, Calum S. Henderson, Alexander C. Pakpour-Tabrizi, and Richard B. Jackman[a]

AFFILIATIONS

London Centre for Nanotechnology and the Department of Electronic and Electrical Engineering, UCL (University College London), 17-19 Gordon Street, London WC1H 0AH, United Kingdom

[a]Author to whom correspondence should be addressed: r.jackman@ucl.ac.uk

ABSTRACT

Surface transfer-doping, involving hydrogen terminated diamond surfaces, has been an effective method for producing diamond devices for some years but suffered from poor device longevity and reproducibility. The emergence of metal oxides as an encapsulant has begun to change this situation. Here, HfO_2 encapsulated surface transfer doped diamond Schottky diodes with stable device characteristics have been demonstrated. Ideality factor and Schottky barrier heights of the devices did not vary considerably across extended periods of use (up to 39 days). The devices showed excellent blocking capabilities, demonstrating no catastrophic breakdown under the maximum field applied and only a slight increase in leakage current at the reverse bias and field strength of 200 V and 0.167 MV cm^{-1}, respectively. Indeed, a large rectification ratio of up to 10^8 and a very low leakage current of $\approx 10^{-9}$ A cm^{-1} were maintained at this reverse bias (200 V). Furthermore, multiple devices were compared across a single substrate, something rarely reported previously for surface transfer doped diamond diodes. Leakage currents and rectification ratios were similar for all of the devices.

The increased use of distributed energy generation facilities calls for ever more energy efficient power switches and inverters. As an ultra-wide bandgap (UWBG) semiconductor, diamond ($E_G \approx 5.5$ eV) is of interest in this context given its high electric breakdown strength, potential for high carrier mobilities, and high thermal conductivity.[1,2] Initial device development was hindered by the availability of suitable high quality diamond substrates, but this problem has been largely overcome[3] and even 2-in. diamond wafers are now emerging.[4] Although n-type doping has been demonstrated, the relatively high activation energy of the phosphorous donors (≈0.6 eV) and the defects induced by the introduction of P atoms into the dense diamond lattice reduce the usefulness of this form of material for electronic devices.[5] Boron doped, p-type, diamond suffers less from these problems ($E_a \approx 0.37$ eV) and has been widely used for fabrication of unipolar diamond devices, although operation at elevated temperatures is often required for optimal performance.[6]

An alternative approach to conventional doping is the introduction of a surface conductive layer[7] through a process often referred to as "surface transfer doping (STD)" of diamond. In this case, a H-terminated diamond surface in the presence of a suitable adsorbate undergoes electron transfer through the C–H polar bond into the adsorbate layer leading to the formation of a hole accumulation layer near the diamond surface.[8] The resultant p-type region can be treated as a 2D-hole-gas (2DHG).[9] This p-type layer forms with little thermal activation ($10 - 40$ meV[10]) compared to 0.37 eV required for activation of boron acceptor states, and the H-termination required also prevents surface states leading to Fermi level pinning, so near-to ideal Schottky barriers' heights can be achieved.[11]

Although this approach can be used to fabricate highly effective diodes and transistors,[12,13] devices suffer from thermal instability and long term performance drift primarily due to the volatility of the adsorbates.[14] The alternative use of thin metal oxide layers has led to significant improvements in device stability. MoO_3 has a high electron affinity of ≈6.7 eV, leading to the conduction band minimum of MoO_3 lying more than 2.8 eV below the H-terminated diamond valence band maximum. This makes electron transfer from the diamond to MoO_3 energetically favorable and enables the process of surface transfer doping to occur without the need of adsorbates.[15] Al_2O_3, V_2O_5, and other metal oxides can be used in a similar fashion.[16–19]

The improvements in device stability that arise from the use of metal oxides have enabled the benefits of STD to be realistically explored for device fabrication. Foremost among these have been

field-effect-transistors (FETs). Metal-semiconductor FETs (MESFETs) have utilized a H-terminated surface, which is directly contacted by a Schottky barrier forming metal; the remaining H-terminated diamond regions between the source and drain contacts are covered with the metal oxide of choice.[20] Alternatively, metal–insulator–semiconductor or metal–oxide–semiconductor FETs (MIS-, MOS-FETs) cover the entire H-terminated diamond with metal oxide prior to source, drain, and gate fabrication.[21] The potential for high switching speeds makes power MESFETs and MOSFETs in demand for microwave applications.[22] In the case of H-diamond MOSFETs, the maximum output current, cutoff frequency (f_T), and microwave output power densities of 1.3 A mm^{-1} at 70 GHz, 3.8 W mm^{-1} at 1 GHz, and 182 W mm^{-1} at 10 GHz, have been demonstrated.[23–26]

In a recent study,[27] Ren and coworkers used x-ray photoelectron spectroscopy to determine that the HfO_2/H-diamond interfacial valence band offset was also particularly large at 1.98 eV. This suggests that this metal oxide should act as a particularly effective dielectric for STD and subsequent MOSFET fabrication. Indeed, they reported Baliga's figure of merit for their devices to be ≈2.0 MW cm^{-2} when using HfO_2 as thin as 28 nm, a value not obtained, for example, with Al_2O_3 without a thickness of 200 nm. This was despite the authors using polycrystalline, rather than single crystal diamond substrates. Thick gate oxides reduce the effectiveness of the gate to modulate the channel.

Power diodes are required as rectifiers, but the specific design of diamond diodes using STD has received less attention than that of FETs. The current study utilizes thin (30 nm) HfO_2 to encapsulate the H terminated diamond channel of Al/H-diamond Schottky barrier diodes. HfO_2 enables effective STD of the regions separating the Schottky from the Ohmic contacts; electronic grade single crystal diamond is used throughout. It is well known that edge-termination effects, which can cause current crowding and early onset breakdown, can be reduced by the use of field plates within the design of the structure.[28] Such an approach has been adopted for boron-doped diamond Schottky diodes.[29] Here, a field plate design is incorporated into HfO_2 encapsulated surface transfer doped diodes.

The implemented design is illustrated in Fig. 1. The top view [Fig. 1(a)] shows the corbino structure adopted where the central Schottky contact (Al) is separated from the adjacent Ohmic contact (Au) by 4 μm. Figure 1(b) shows the design in cross section. H-terminated diamond interfacial regions are isolated using O-terminated interfaces, such that parts of the Ohmic and Schottky metalization and the HfO_2 layer are deposited on H-terminated diamond. These regions affect the STD process. Central and outer edge regions of Au and Al are deposited on O-terminated diamond as is an outer ring of HfO_2. Hence, in this device, the entire surface was O-terminated except a 35 μm hydrogen "channel." This approach not only enables device isolation but also improves adhesion of the metal layers to the single crystal diamond surfaces. The latter arises since the metals can partially react with the O-terminated regions for good adhesive properties, while a small area is still active for STD in the H-terminated regions.

Experimentally, electronic grade single crystal diamond (B < 1ppb, N < 10ppb, R_a < 3nm, Chenguang Machinery Ltd.) was used throughout. Samples were cleaned by submerging in an acid etching solution [H_2SO_4 : $(NH_4)_2S_2O_8$, at 200°C, 20 min] followed by submersion in an alkaline solution (H_2O_2 : NH_4OH, 10 min). This

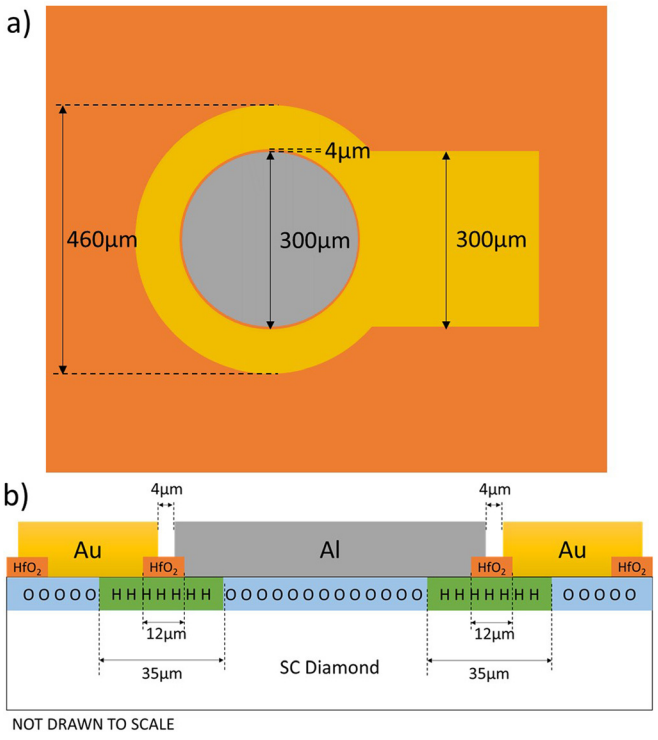

FIG. 1. (a) A cross-sectional view of the HfO_2 encapsulated corbino-style Schottky diodes. (b) A side cross section of the devices showing the field plate architecture and device isolation.

process ensured the removal of any graphitic carbon and provides a hydrocarbon-free, partly oxidized surface.[30] Substrates were then exposed to ozone (200 °C, 1 h) to ensure complete O-termination was achieved. Selective hydrogenation was then performed; first a 200 nm thick Al layer was deposited by thermal evaporation and patterned by wet etching to achieve an Al hard mask. The exposed areas were then exposed to a hydrogen plasma for 15 min in Astex PDS18 with the pressure, power, and substrate temperature of 62 Torr, 1500 W, and 450 °C, respectively. A 30 nm HfO_2 layer was deposited by atomic-layer deposition (ALD, Ultratech, Savannah G2 S200) using TDMAH (heated to 75 °C) and water vapor precursors and a substrate temperature of 150 °C, and patterned by lift off. This covered 12 of the 35 μm hydrogenated region [as shown in Fig. 1(b)]. Next, the 350 nm thick Al Schottky and 250 nm thick Au Ohmic contacts were deposited separately by thermal evaporation (Edwards A306 box and E306 bell jar) and patterned by lift off. Since H termination of the diamond surface is known to prevent Fermi-level pinning, an Ohmic contact can be formed through the choice of a suitable metal work function without the need for a reacted type interface such as arises with the use of, for example, Ti.[31] Photo-lithographic patterning was performed throughout using a direct-write prototyping tool (Heidelberg DWL 66+).

I–V (current–voltage) and C–V (capacitance–voltage) measurements were performed using a Keithley 4200 semiconductor characterization system along with an Evergreen probe station (Evergreen EB-6 DC, supplied by Lambda Photometrics Ltd). Figure 2(a) shows logarithmic current plotted against applied voltage in both forward

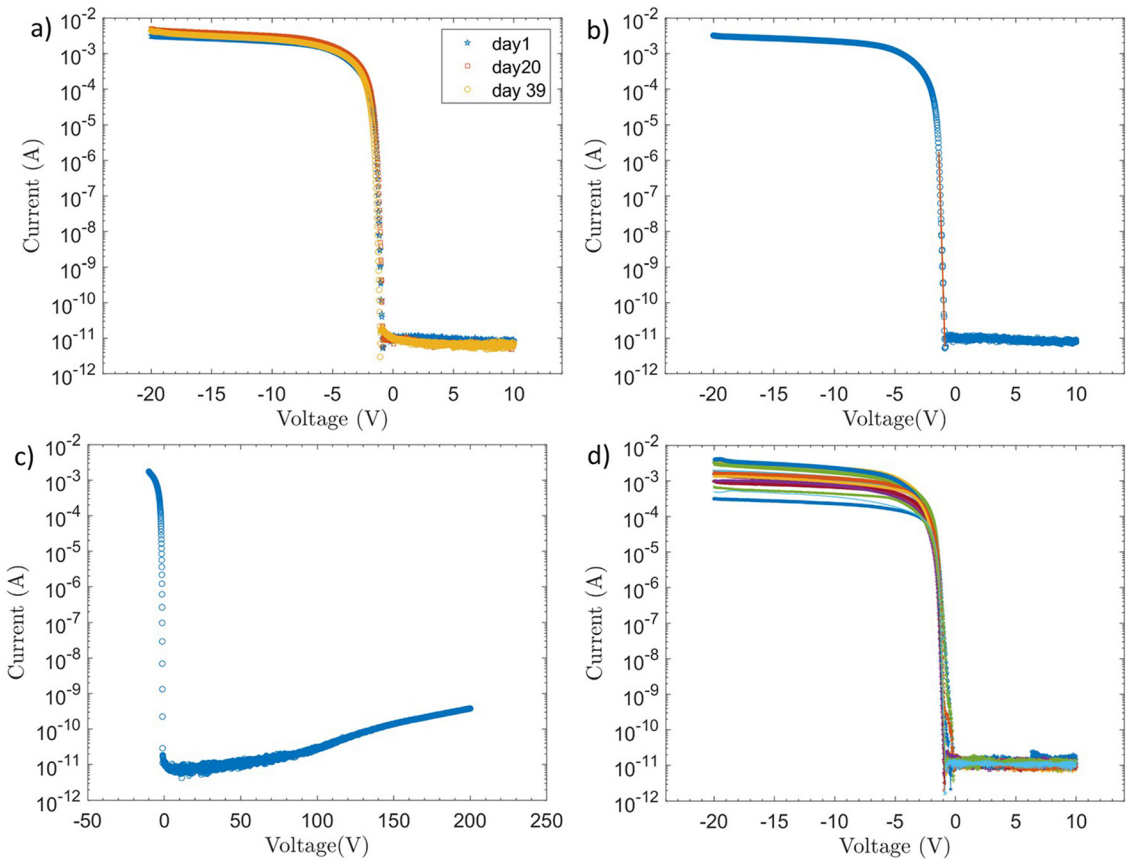

FIG. 2. (a) Current voltage characteristics for HfO_2 encapsulated Schottky diodes on day 1 after fabrication, day 20 and day 39;(b) thermionic emission theory has been fitted to the linear section of the log IV curve for the same device on day 1 to achieve $n = 1.6$ and $\Phi_B = 1.35$ eV; (c) the reverse breakdown characteristics of the same device on day 39 are presented; and (d) the I–V characteristics for 13 devices across a single substrate are presented.

and reverse bias conditions. It is apparent that the device is highly rectifying with ratio $>10^8$. Over this voltage range, the leakage current is extremely low, being similar to the noise limit of the measuring instrument. In forward bias, the current appears to approach saturation at a value of 5×10^{-3} A. If the diode perimeter is considered to be the active device region for current flow then this is equivalent to 0.05 A cm^{-1}. To evaluate the stability of the devices, a device was repeatedly scanned over a period extending up to 39 days. No significant variation in either forward or reverse bias characteristics resulted, as shown in Fig. 2(a), where measurements for days 1, 20, and 39 are shown.

It is well documented that the dominant mechanism for current flow in a Schottky diode at forward bias is thermionic emission.[32] In Fig. 2(b), the linear region of ln(I) when plotted against V is clearly visible, enabling the ideality factor, n, and Schottky barrier height, Φ_B, to be derived from the gradient and y intercept of the graph. n and Φ_B were found to be 1.57 and 1.37 eV, respectively, for the day 1 data, and little changed thereafter. The band structure expected for H-terminated diamond surfaces in contact with various metal oxides has recently been reviewed;[9] in the current case, the use of HfO_2 fits the expected pattern of STD needing high electron affinity metal oxides. While the degree of upward band bending induced by charge transfer through the C-H layer into the metal oxide should relate directly to the electronegativity of the metal oxide chosen, this relationship has been found to be overly simplistic. For example, variations in the adsorbate state of the diamond surface prior to metal oxide deposition and stoichiometric nature of the oxide being implicated. Furthermore, Al_2O_3, which is insufficiently electronegative to expect STD to be effective, has controversially been found to capable of supporting STD.[17] It is clear that an exact band picture for the process of STD with metal oxides has yet to emerge.

Figure 2(c) shows an I–V plot for higher reverse bias values, up to the 200 V limit of the measurement system in use. Although some "soft" increase in the reverse bias leakage current is apparent, no catastrophic breakdown occurs. The device could be repeatedly operated over this electric-field regime without any significant degradation in I–V characteristics. At the maximum field strength applied here (0.167 MV cm^{-1}), a rectification ratio of $>10^7$ persists with a leakage current of only $\approx 10^{-9}$ Acm^{-1}. The field strength was calculated by dividing the voltage by the channel length, which is considered to be the width of the HfO_2 layer. The active area that should be attributable to the current device, based upon the method of STD as it is, remains controversial.[9] It seems reasonable to take this value to be the area of the circular "ring" of HfO_2 that is in contact with the H-terminated

diamond surface. On this basis, Baliga's figure-of-merit (FOM)[33] gives a value of around 2.1 MW cm^{-2}. In comparison, a similar calculation for a conventionally boron doped pseudo-vertical device has been reported as significantly higher at 244 MW cm^{-2}.[34] This device was based on the P++/P- stack with Zr/Pt/Au Schottky contacts. However, it should be noted that in the current case, the device active area has not been optimized for maximum contact area. Moreover, the reverse bias used has yet to reveal significant breakdown, suggesting that the device is capable of supporting higher voltages under appropriate experimental conditions. Since Baliga's FOM is influenced by both the maximum applied voltage with the relation $(V_{max})^2$ and the contact area, this FOM should be taken as a lower limit for this type of device. Of course, a lateral device, based upon 2D-like STD, will never offer the power handling capability of a vertical device technology, although it offers other advantages such as simplicity of integration with other lateral device structures.

An important parameter for the application of a device technology is the variability of I–V characteristics of nominally similar devices across a given substrate; such data are often missing from published studies involving diamond devices based upon STD. Figure 2(d) shows the I–V plots for 13 different devices measured across the same fabricated "chip." While some variation is apparent in the forward bias characteristics, the reverse bias data show no significant variation.

Figure 3 shows the reverse bias C–V characteristics of these Schottky diodes, measured while applying AC voltage frequencies ranging between 200 kHz and 1 MHz. The plot shows the value of measured capacitance (pF) plotted against the applied bias on the device. The C–V curves show plateau effect in the reducing capacitance as the voltage is increased before again the capacitance values reduce. This is the same for all frequencies tested, although a slight variation in the actual capacitance value measured around 1.5 V can be observed.

The design implemented here employs metallization schemes (both Ohmic and Schottky) directly contacting H-terminated diamond, along with regions of both contacting HfO_2 on H-terminated diamond. Such that the Al/H-diamond interface induces Schottky

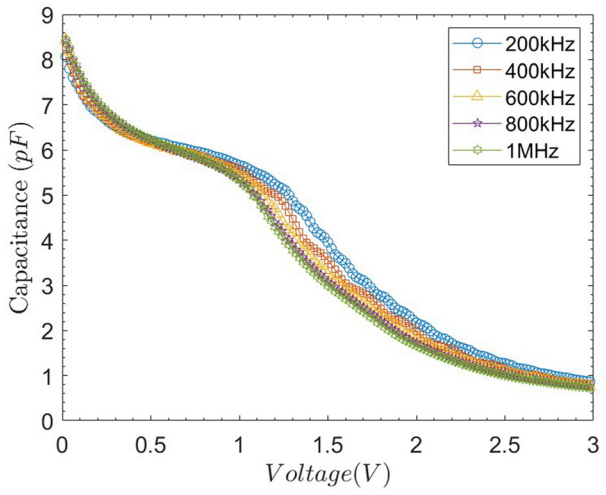

FIG. 3. Capacitance–voltage characteristics for varying AC voltages from 200 kHz to 1 MHz.

diode characteristics, the Al/HfO_2/H-diamond interface induces MOS characteristics and the HfO_2 encapsulated channel induces the STD effect. The localization of the surface H-terminated region within O-terminated diamond enables effective device isolation and was found to aid the adhesion of the metal layers onto the smooth ($R_a \approx 3$ nm) single crystal diamond surfaces. Furthermore, the implemented field-plate design allowed minimization of current crowding near the otherwise field enhanced edges of the metallization. This design gives rise to Schottky diodes with high rectification ratio and only modest increases in reverse bias leakage currents and no-apparent hard-breakdown over the field strengths measured.

Furthermore, it should be noted that the device performance barely changes over the investigated period of 39 days. Device longevity is poorly reported in the literature. However, in the previous work,[35] the stability of the metal-oxide induced surface transfer doping on diamond has been investigated using Hall measurements. The carrier density was shown to remain consistent for MoO_3 and V_2O_5 across a 17 day period with a 400 °C anneal prior to deposition by thermal evaporation. However, a 400 °C anneal is not always practical if working with photo-resists for further processing. The carrier density was also measured in Ref. 18 without the anneal prior to deposition and shown to decay over a period of 17 days for both MoO_3 and V_2O_5 and would be expected to have continued to decay over longer time periods. In this work, HfO_2 was deposited by ALD with an anneal of only 150° for approximately 15 min prior to deposition and a consistent current over 39 days is demonstrated in Fig. 2(a), demonstrating the ability to achieve stable surface transfer doping without a high temperature anneal, using ALD.

Due to the field plate design chosen for these devices, two curves can be observed in the CV plot (Fig. 3). It is likely that different CV characteristics will arise due to the different interfaces present in the devices architecture. When the Al contact is touching the H-terminated diamond surface directly, the device will exhibit diode-like CV characteristics. However, in the field plate region of the device, a MOS capacitance will be present, since Al is separated from the H-terminated diamond surface by the HfO_2 layer. This creates more complex CV characteristics, which are difficult to model. The region of the graph between 2 and 3 V appears very similar to CV characteristics presented by Garrido *et al.*,[35] wherein CV characteristics were studied for air encapsulated surface transfer doped diamond Schottky diodes with different Schottky contact areas. In such a case, it was suggested that as the depletion region extends into the channel of the device, the CV graph begins to exhibit more typical Schottky diode characteristics.

To conclude, HfO_2 encapsulated surface transfer doped diamond Schottky diodes with stable device characteristics have been demonstrated. Ideality factor, n, and Schottky barrier height, Φ_B, of the devices did not vary considerably across extended periods of use (up to 39 days). The devices showed excellent blocking capabilities, demonstrating only minor soft breakdown occurring at a reverse bias and field strength of 200 V and 0.167 MV cm^{-1} with a large rectification ratio of up to 10^8, and a very low leakage current of $\approx 10^{-9}$ Acm^{-1} at a reverse bias of 200 V. Future studies are planned using higher voltage capable equipment and packaging to determine an ultimate breakdown field for these devices.

Furthermore, multiple devices were compared across a single substrate, something rarely reported previously for STD diamond

diodes. Leakage currents and rectification ratios were similar for all of the devices. Some variation in the forward current was apparent. This could be due to experimental variation in the mechanical probing process between devices or perhaps due to sheet carrier concentration changes across the substrate caused by local variations in crystal surface quality or crystal polish conditions.

Capacitance–voltage studies were also performed that demonstrated the complex structure of these devices with two regions being apparent in the reverse bias. These were thought to be due to the incorporated field plate creating MOS characteristics appearing alongside typical Schottky diode characteristics.

This work shows the value of careful metal oxide and substrate selection and the use of designs incorporating field-plates in achieving high performance diamond diodes. Not only do these devices perform well on day 1 but continue to offer outstanding characteristics for periods greater than one month. Furthermore, reasonable device reproducibility over a single crystal diamond chip has been shown to be achievable.

The authors are grateful to the UKs Engineering and Physical Sciences Research Council (EPSRC) and BAE Systems Marine Ltd. for the award of a "Cooperative Awards in Science and Engineering (CASE)" Ph.D. Studentship for R.J.W. and to EPSRC for the award of related research funding (No. EP/H020055/1). A.C.P.-T. and R.B.J. also acknowledge invaluable assistance, both financial and in the form of international collaborations, from the European Commission Horizon 2020 Project "GREENDIAMOND" (H2020 Large Project under Grant No. SEP-210184415). Lambda Photometrics Ltd. and Everbeing International Corporation are gratefully acknowledged for use of a Everbeing EB-6 DC probe station. Finally, the LCN Cleanroom is acknowledged for the invaluable assistance of technicians and for the use of the ALD, evaporation, and photo-lithography tools.

AUTHOR DECLARATIONS

Conflict of Interest

The authors have no conflicts to disclose.

Author Contributions

Rebecca Jane Watkins: Data curation (lead); Formal analysis (equal); Investigation (lead); Methodology (equal); Validation (equal); Writing – original draft (equal); Writing – review & editing (equal). **Calum S. Henderson:** Investigation (equal); Methodology (equal); Writing – review & editing (equal). **Alexander C. Pakpour-Tabrizi:** Conceptualization (equal); Methodology (equal); Supervision (equal); Writing – review & editing (equal). **Richard B. Jackman:** Conceptualization (lead); Formal analysis (equal); Funding acquisition (lead); Methodology (lead); Project administration (lead); Resources (lead); Supervision (lead); Writing – original draft (equal); Writing – review & editing (equal).

DATA AVAILABILITY

The data that support the findings of this study are available within the article.

REFERENCES

[1]M. Geis, "Growth of device-quality homoepitaxial diamond thin films," in *MRS Online Proceedings Library (OPL)* (Cambridge University Press, 1989), p. 162.
[2]E. Wörner, C. Wild, W. Müller-Sebert, R. Locher, and P. Koidl, "Thermal conductivity of CVD diamond films: High-precision, temperature-resolved measurements," Diamond Relat. Mater. **5**, 688 (1996).
[3]J.-C. Arnault, S. Saada, and V. Ralchenko, "Chemical vapor deposition single-crystal diamond: A review," Phys. Status Solidi RRL **16**, 2100354 (2022).
[4]S.-W. Kim, R. Takaya, S. Hirano, and M. Kasu, "Two-inch high-quality (001) diamond heteroepitaxial growth on sapphire (110) misoriented substrate by step-flow mode," Appl. Phys. Express **14**, 115501 (2021).
[5]S. Koizumi and M. Suzuki, "n-Type doping of diamond," Phys. Status Solidi A **203**, 3358–3366 (2006).
[6]J. Cañas, A. C. Pakpour-Tabrizi, T. Trajkovic, F. Udrea, D. Eon, E. Gheeraert, and R. B. Jackman, "Normally-OFF diamond reverse blocking MESFET," IEEE Trans. Electron Devices **68**, 6279–6285 (2021).
[7]H. Looi, L. Pang, A. Molloy, F. Jones, J. Foord, and R. Jackman, "An insight into the mechanism of surface conductivity in thin film diamond," Diamond Relat. Mater. **7**, 550–555 (1998).
[8]P. Strobel, M. Riedel, J. Ristein, and L. Ley, "Surface transfer doping of diamond," Nature **430**, 439–441 (2004).
[9]K. G. Crawford, I. Maini, D. A. Macdonald, and D. A. Moran, "Surface transfer doping of diamond: A review," Prog. Surf. Sci. **96**, 100613 (2021).
[10]O. A. Williams, M. D. Whitfield, R. B. Jackman, J. S. Foord, J. E. Butler, and C. E. Nebel, "Carrier generation within the surface region of hydrogenated thin film polycrystalline diamond," Diamond Relat. Mater. **10**, 423–428 (2001).
[11]K. Tsugawa, H. Noda, K. Hirose, and H. Kawarada, "Schottky barrier heights, carrier density, and negative electron affinity of hydrogen-terminated diamond," Phys. Rev. B **81**, 045303 (2010).
[12]R. B. Jackman, H. J. Looi, L. Y. Pang, M. D. Whitfield, and J. S. Foord, "High-performance devices from surface-conducting thin-film diamond," Carbon **37**, 817 (1999).
[13]S. P. Lansley, H. J. Looi, Y. Wang, M. D. Whitfield, and R. B. Jackman, "A thin-film diamond phototransistor," Appl. Phys. Lett. **74**, 615–617 (1999).
[14]J. S. Foord, C. H. Lau, M. Hiramatsu, R. B. Jackman, C. E. Nebel, and P. Bergonzo, "Influence of the environment on the surface conductivity of chemical vapor deposition diamond," Diamond Relat. Mater. **11**, 856–860 (2002).
[15]S. A. Russell, L. Cao, D. Qi, A. Tallaire, K. G. Crawford, A. T. Wee, and D. A. Moran, "Surface transfer doping of diamond by MoO_3: A combined spectroscopic and Hall measurement study," Appl. Phys. Lett. **103**, 202112 (2013).
[16]K. G. Crawford, L. Cao, D. Qi, A. Tallaire, E. Limiti, C. Verona, A. T. Wee, and D. A. Moran, "Enhanced surface transfer doping of diamond by V_2O_5 with improved thermal stability," Appl. Phys. Lett. **108**, 042103 (2016).
[17]C. Verona, W. Ciccognani, S. Colangeli, E. Limiti, M. Marinelli, and G. Verona-Rinati, "Comparative investigation of surface transfer doping of hydrogen terminated diamond by high electron affinity insulators," J. Appl. Phys. **120**, 025104 (2016).
[18]K. G. Crawford, D. Qi, J. McGlynn, T. G. Ivanov, P. B. Shah, J. Weil, A. Tallaire, A. Y. Ganin, and D. A. Moran, "Thermally stable, high performance transfer doping of diamond using transition metal oxides," Sci. Rep. **3**, 3342 (2018).
[19]M. Tordjman, K. Weinfeld, and R. Kalish, "Boosting surface charge-transfer doping efficiency and robustness of diamond with WO_3 and ReO_3," Appl. Phys. Lett. **111**, 111601 (2017).
[20]K. G. Crawford, J. D. Weil, P. B. Shah, D. A. Ruzmetov, M. R. Neupane, K. Kingkeo, A. G. Birdwell, and T. G. Ivanov, "Diamond field-effect transistors with V_2O_5-induced transfer doping: Scaling to 50-nm gate length," IEEE Trans. Electron Devices **67**, 2270–2275 (2020).
[21]A. Vardi, M. Tordjman, J. A. del Alamo, and R. Kalish, "A diamond: H/MoO_3 MOSFET," IEEE Electron Device Lett. **35**, 1320–1322 (2014).
[22]T. Weatherford, D. McMorrow, W. Curtice, A. Knudson, and A. Campbell, "Single event induced charge transport modeling of GaAs MESFETs," IEEE Trans. Nucl. Sci. **40**, 1867–1871 (1993).
[23]K. Hirama, H. Sato, Y. Harada, H. Yamamoto, and M. Kasu, "Diamond field-effect transistors with 1.3 A/mm drain current density by Al_2O_3 passivation layer," Jpn. J. Appl. Phys., Part 1 **51**, 090112 (2012).

[24]X. Yu, J. Zhou, C. Qi, Z. Cao, Y. Kong, and T. Chen, "A high frequency hydrogen-terminated diamond MISFET with f_T/f_{max} of 70/80 GHz," IEEE Electron Device Lett. **39**, 1373–1376 (2018).
[25]S. Imanishi, K. Horikawa, N. Oi, S. Okubo, T. Kageura, A. Hiraiwa, and H. Kawarada, "3.8 W/mm RF power density for ALD Al_2O_3-based two-dimensional hole gas diamond MOSFET operating at saturation velocity," IEEE Electron Device Lett. **40**, 279–282 (2019).
[26]X. Yu, J. Zhou, S. Zhang, Z. Cao, Y. Kong, and T. Chen, "High frequency H-diamond MISFET with output power density of 182 mW/mm at 10 GHz," Appl. Phys. Lett. **115**, 192102 (2019).
[27]Z. Ren, Y. Xing, D. Lv, J. Xu, J. Zhang, J. Zhang, K. Su, C. Zhang, H. Zhang, Q. He *et al.*, "H-diamond MOS interface properties and FET characteristics with high-temperature ALD-grown HfO_2 dielectric," AIP Adv. **11**, 035041 (2021).
[28]Y. Ando, Y. Okamoto, H. Miyamoto, T. Nakayama, T. Inoue, and M. Kuzuhara, "10-W/mm AlGaN-GaN HFET with a field modulating plate," IEEE Electron Device Lett. **24**, 289–291 (2003).
[29]K. Ikeda, H. Umezawa, and S. Shikata, "Edge termination techniques for p-type diamond Schottky barrier diodes," Diamond Related Mater. **17**, 809–812 (2008).
[30]B. Baral, S. S. Chan, and R. B. Jackman, "Cleaning thin-film diamond surfaces for device fabrication: An Auger electron spectroscopic study," J. Vac. Sci. Technol. A **14**, 2303 (1996).
[31]H. J. Looi, M. D. Whitfield, J. S. Foord, and R. B. Jackman, "The effect of hydrogen on the electronic properties of CVD diamond films," Thin Solid Films **343**, 623–626 (1999).
[32]E. H. Rhoderick, "Metal-semiconductor contacts," IEE Proc. I **129**, 1–14 (1982).
[33]B. J. Baliga, "Power semiconductor device figure of merit for high-frequency applications," IEEE Electron Device Lett. **10**, 455–457 (1989).
[34]A. Traoré, P. Muret, A. Fiori, D. Eon, E. Gheeraert, and J. Pernot, "Zr/oxidized diamond interface for high power schottky diodes," Appl. Phys. Lett. **104**, 052105 (2014).
[35]J. A. Garrido, C. E. Nebel, M. Stutzmann, E. Snidero, and P. Bergonzo, "Capacitance–voltage studies of Al-Schottky contacts on hydrogen-terminated diamond," Appl. Phys. Lett. **81**, 637–639 (2002).